

UNCLASSIFIED

AD 4 6 4 6 3 5

DEFENSE DOCUMENTATION CENTER

FOR

SCIENTIFIC AND TECHNICAL INFORMATION

CAMERON STATION ALEXANDRIA, VIRGINIA



UNCLASSIFIED

NOTICE: When government or other drawings, specifications or other data are used for any purpose other than in connection with a definitely related government procurement operation, the U. S. Government thereby incurs no responsibility, nor any obligation whatsoever; and the fact that the Government may have formulated, furnished, or in any way supplied the said drawings, specifications, or other data is not to be regarded by implication or otherwise as in any manner licensing the holder or any other person or corporation, or conveying any rights or permission to manufacture, use or sell any patented invention that may in any way be related thereto.

ATD Report P-65-33

25 May 1965

Surveys of Soviet-Bloc Scientific and Technical Literature

CATALOGED BY: DDC

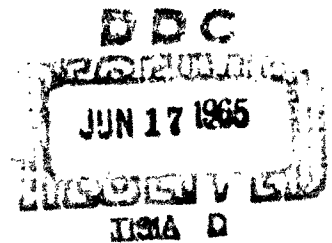
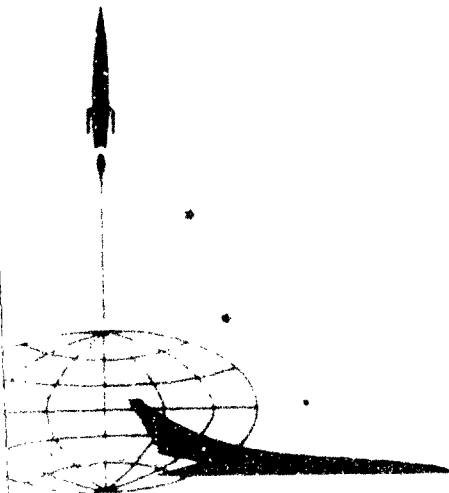
464635

464635

**MIXING OF CONCENTRIC HIGH-VELOCITY
AIR STREAMS**

Compilation of Abstracts

(Report No. 3 in this series)



Aerospace Technology Division
Library of Congress

Surveys of Soviet-Bloc Scientific and Technical Literature

MIXING OF CONCENTRIC HIGH-VELOCITY AIR STREAMS

Compilation of Abstracts

(Report No. 3 in this series)

The publication of this report does not constitute approval by any U. S. Government organization of the inferences, findings, and conclusions contained herein. It is published solely for the exchange and stimulation of ideas.

Aerospace Technology Division
Library of Congress

FOREWORD

This report, prepared in response to ATD Work Assignment No. 60, is the third in a series dealing with published Soviet research on the subject of the mixing of concentric high-velocity airstreams. It comprises abstracts of articles selected from Soviet open literature available at the Aerospace Technology Division and the Library of Congress.

Full translations of some of the source materials used in this report may be available from other agencies or commercially. Interested readers may obtain translation data for individual sources by indicating source numbers from the bibliography list on the form attached at the end of this report and returning it to the Aerospace Technology Division.

MIXING OF CONCENTRIC HIGH-VELOCITY AIRSTREAMS

1. Bezmenov, V. Ya., and V. S. Borisov. Turbulent air jets heated to 4000°K. IN: Akademiya nauk SSSR. Izvestiya. Otdeleniye tekhnicheskikh nauk. Energetika i avtomatika, no. 4, 1961, 42-45.

Experiments were carried out with free, high-temperature submerged air jets to verify various hypotheses concerning the effect of jet temperature on the width of the mixing zone, change in parameters along the jet axis, and positions of the jet outer boundaries.

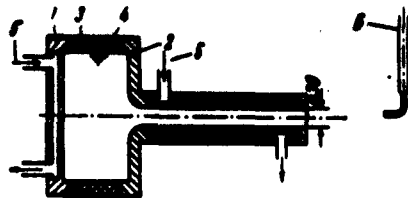


Fig. 1. Diagram of the experimental unit

1 - cathode; 2 - anode; 3 - insulator; 4 - cold air inlet; 5 - water cooling inlet; 6 - measuring attachment.

The experiments were carried out in an experimental unit (Fig. 1) in which an electric arc is used to attain temperatures up to 4000°K corresponding to a density ratio of $\rho_2/\rho_1 = 14$ (where ρ_2 is the air density in the inlet section of the jet and ρ_1 is the density of the surrounding media). The nozzle exit temperature was maintained in the range of 1000—1600°C. The relative velocity head (p) and the relative excess temperature [superheat] (v) were determined as a function of x/d (distance between the cross sections investigated and the nozzle diameter d) and are shown in Figs. 2 and 3, where:

$$p = \rho_m u_m^2 / \rho_0; u_m^2 \text{ and } v = t_m - t_a / t_{\text{mean}} = t_a$$

($1/2 \rho_0 m u_m^2$ is the maximum velocity head, t_{mean} is the mean temperature at the exit from the heating chamber, t_a is the temperature of the

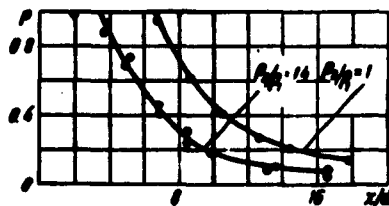


Fig. 2. Change in the relative velocity head p on u_m^2 along the jet axis

○ - experiments at $\rho_2/\rho_1 = 1$,
● - $\rho_2/\rho_1 = 14$.

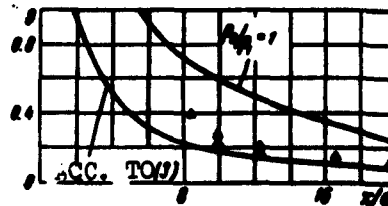


Fig. 3. Change in the relative maximum excess temperature $t_m - t_a / t_{\text{mean}} - t_a$ along the jet axis

▲ - experiments at $\rho_2/\rho_1 = 14$

surrounding medium, and t_m is the maximum temperature). Fig. 3 includes theoretical data obtained with the use of a published equation for calculating the jet mixing zone (Abramovich, G. N., *Teoriya turbulentnykh struy*, 1960):

$$u = \int_0^b \rho u dx / \int_0^b \rho dy$$

It is shown that the values of both the length of the initial zone and the width of the mixing zone obtained in the experiments differ considerably from the calculated values. This is attributed to the fact that 1) the theory is based on the assumption that the heat capacity of air in nonisothermal jets is constant, which is incorrect in the case considered, and 2) the true dependence of the width of the mixing zone on the ρ_2/ρ_1 ratio is not sufficiently reflected in the equation. Theoretical and experimental distribution curves of dimensionless velocities and temperatures across the jet show that the theory is in satisfactory agreement with the experiment.

2. Ginevskiy, A. S. Turbulent wake and jet in a concurrent stream in the presence of the longitudinal pressure gradient. IN: *Akademiya nauk SSSR. Izvestiya. Otdeleniye tekhnicheskikh nauk. Mekhanika i mashinostroyeniye*, no. 2, 1959, 31-36.

A approximate method is proposed for calculating the free turbulence in the presence of the longitudinal pressure gradient in concurrent streams. The method is based on the representation of the tangential stress profile in the jet or wake as a polynomial ($\tau = B_0 + B_1 y + B_2 y^2$), whose coefficients are determined from the boundary conditions on the jet axis and boundaries, using the differential equations of motion. The profile so determined is the result of motion and is not connected with any assumptions concerning the mechanism of motion. A series of mathematical transformations leads to the following equation for dimensionless profiles for both jet and wake in a concurrent flow:

$$u^0 = u_m^0 + (1 - u_m^0) F(y^0), \quad (1)$$

$$u^0 = u/U, \quad u_m^0 = u_m/U,$$

where $F(y^0) = \frac{8}{\pi} \left\{ \left(\frac{1}{2} - y^0 - \frac{1}{4} \right) \sqrt{y^0 - y^0} + \frac{1}{2} \arcsin(2y^0 - 1) \right\}$,

u is the average velocity along the jet axis, U is the velocity of the outer flow, and $y^0 = y/\delta$ (see Fig. 4, a and b). Considering that $u = U \frac{u_1}{u_m}$ and $u_m = U \frac{u_{1m}}{u_m}$, the deficiency or excess velocity is expressed by the following equation:

$$u_1/u_{1m} = 1 - F(y^0). \quad (2)$$

Thus, the longitudinal pressure gradient in the region of wake or jet in a concurrent flow has no effect on the shape of the velocity

profile; it affects only the law of the variation in the velocity and the width of the wake or jet along its axis. A series of equations was derived and solved for various cases and conditions, including the case of plane wake:

$$u_{1m} = \frac{\pi}{163} \sqrt{c_x L} s^{-1/2}, \quad \delta_{1/2} = \frac{2}{L} = \frac{4\beta}{\pi} \sqrt{s \frac{\pi}{L}} \quad (3)$$

and the case of a submerged jet ($U = 0$):

$$u_{1m} = \frac{\pi \sqrt{11\beta}}{8 \sqrt{1.4\beta}} s^{-1}, \quad \delta_{1/2} = \frac{2\beta^2}{\pi^2} s \quad (4)$$

The following simplified expressions were obtained for the velocity profiles in a wake or a jet in a concurrent flow:

$$\frac{u_1}{u_{1m}} = 1 - 3y^2 + 2y^4, \quad (5)$$

and

$$\frac{u_1}{u_{1m}} = 1 - 6y^2 + 8y^4 - 3y^6. \quad (6)$$

Velocity profiles obtained according to equations 2, 5, and 6 (see Fig. 5, curves 1, 2, and 3) were compared with those obtained according to previously published experimental data (Fig. 5, curve 4 for the plane turbulent wake; 5 for the plane turbulent jet; 6 for the axisymmetrical turbulent wake; and 7 for the axisymmetrical turbulent jet). The theory, particularly equation 6, is in good agreement with the experiment. The comparison showed that the proposed method may be easily generalized for axisymmetrical free turbulence.

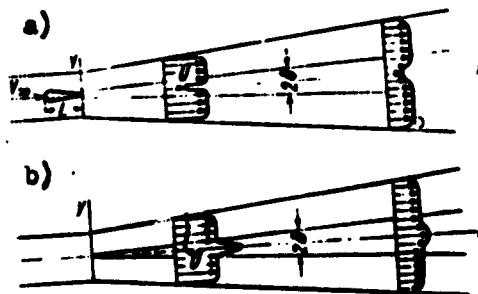


Fig. 4. The effect of the longitudinal pressure gradient on the flow

a - In a turbulent wake, b - in a turbulent jet in a diffuser

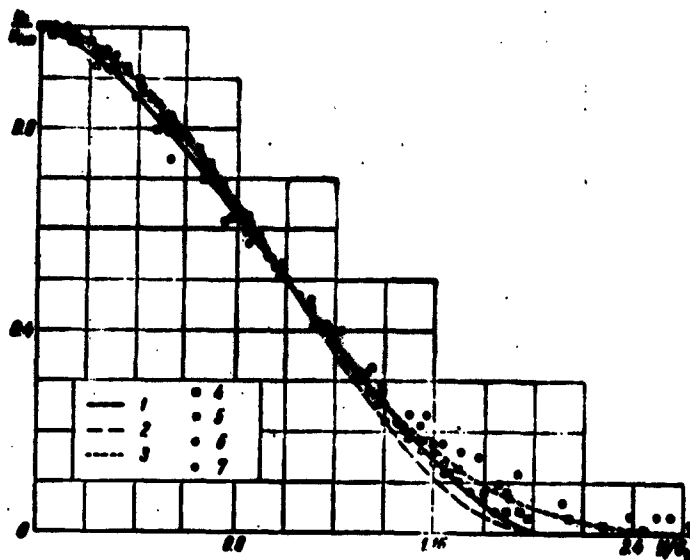


Fig. 5. Calculated and experimental velocity profiles of turbulent wake and jet in a concurrent flow in the presence of longitudinal pressure gradient

3. Ivanov, Yu. V., Kh. N. Suy, and E. P. Timma. A turbulent isothermal jet in a concurrent flow. *Inzhenerno-fizicheskiy zhurnal*, v. 1, no. 5, 1958, 3-10

A review of previous studies on the change in axial velocity of an isothermal cylindrical jet developing in a concurrent flow at $\lambda = v_2/v_1 = 2$ (where v_2 and v_1 are the velocities of the jet and the receiving flow, respectively) showed a marked disagreement between the existing theories (see Fig. 6). To evaluate the existing theories, the axial velocity of an isothermal cylindrical jet developing in a concurrent flow was measured in a horizontal wind tunnel (700 mm in diameter and 2200 mm long) in which jets were generated by a centrifugal fan through nozzles 10.2 and 20.2 mm in diameter. A velocity ratio of $\lambda = 20$ was maintained by decreasing v_1 to ~ 4 m/sec, with a maximum v_2 of about 90 m/sec. The experimental data were treated in the v_m/v_0 and ax/d coordinated (where v_m is the maximum axial velocity in a given cross section, a is the previously postulated jet structure coefficient, and v_0 is a maximum velocity in the jet throat). The experimental curves (Fig. 7) are described by the following derived equation:

$$\frac{v_m}{v_0} = \frac{0,435}{\frac{ax}{d} - 0,15 + \frac{2,2}{\lambda^2 - 1}} + \frac{0,8}{\lambda - 0,2} \quad (1)$$

A comparison of the experimental data with published theories (see Fig. 8) showed that at $\lambda > 5$, the equations proposed by Abramovich

(Izvestiya AN SSSR. Otdeleniye tekhnicheskikh nauk, no. 6, 1957) and by Vulis and Leont'yev (Izvestiya Akademii nauk Kazakhskoy SSR. Seriya energeticheskaya, no. 1, 1957), which were derived by the superposition of motion method, give the closest agreement with the experiment. Experimental studies of plane jets were also carried out in the same experimental unit by replacing the annular nozzles with plane nozzles of various sizes. The results are satisfactorily described by the proposed equation:

$$\frac{v_m}{v_0} = \frac{1,95 - \frac{0,14}{\lambda^{0,3} - 1,28}}{\left(\frac{ax}{b_0} + 3\right)^{0,7}} + \frac{0,7}{\lambda - 0,29} + 0,05, \quad (2)$$

The experimental data obtained are in disagreement with those calculated by the equation for plane isothermal jets in a concurrent flow (A. S. Weinstein, J. F. Osterle, W. Forstall, J. of Applied Mechanics, v. 23, no. 3, 1956). The experimental data at $7 < ax/b_0 < 57$, when $\lambda = 5$, are in good agreement with those calculated by the following equation derived on the basis of the Vulis and Leont'yev equation for the velocity profile of a plane jet in a concurrent flow:

$$\frac{v_m}{v_0} = \frac{1,2(1 - \mu)}{\sqrt{\frac{ax}{b_0} + 0,41}} + \mu, \quad (3)$$

where b_0 is the half-width of the stream and $\mu = 1/\lambda$.

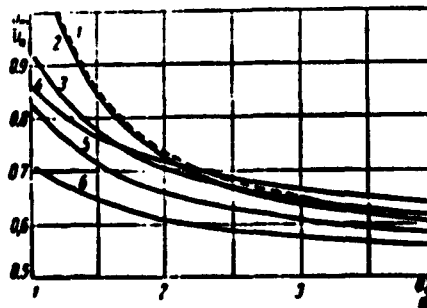


Fig. 6. Change in axial velocity of a jet developing in a concurrent flow at $\lambda = 2$

- 1 - Abramovich ($n_{1u} = n_{2u} = 1$);
- 2 - the same at $n_{1u} \neq n_{2u} \neq 1$;
- 3 - Kyukheman and Veber; 4 - Squire and Troncner; 5 - Squire;
- 6 - Vulis and Leont'yev.

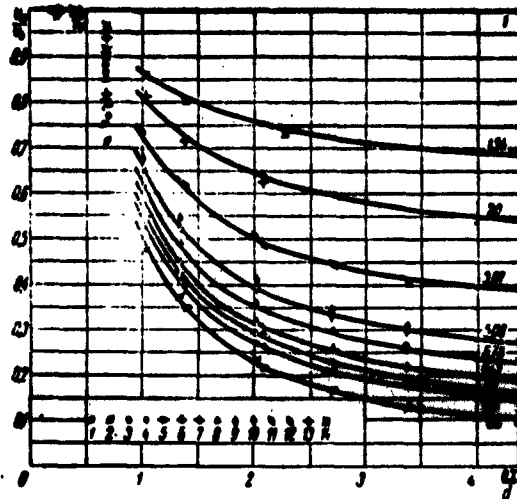


Fig. 7. Relationship between v_m/v_0 and the criterion ax/A at λ ranging from 1.5 to ∞

Curves correspond to equation 1; the figures indicate experimental points 1, 3, 5, 7, 8, 10, and 11 at $a = 0.069$; experimental points 2, 4, 6, 12, 13, and 14 at $a = 0.071$.

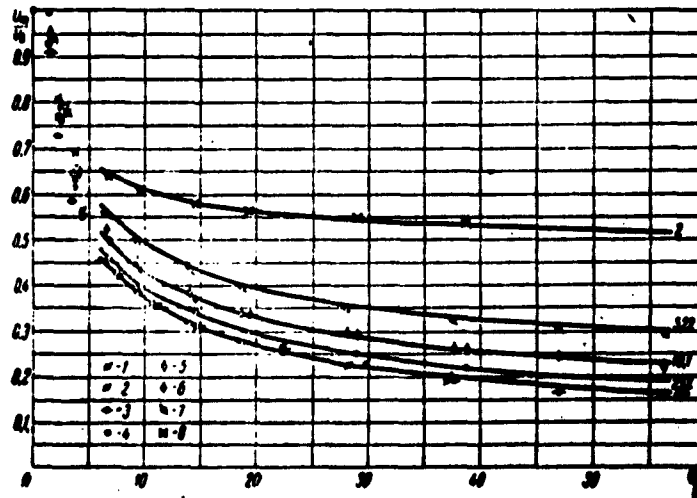


Fig. 8. Relationship between v_m/v_0 and ax/b_0 at λ ranging from 2 to ∞

Curves correspond to equation 3, where figures denote λ . For experimental points 1, 2, 4, 6, and 8, $a = 0.097$, $2b_0 = 2.6$; for experimental points 3, 5, and 7, $a = 0.097$, $2b_0 = 1.2$.

4. Koryavov, P. P. Numerical calculation of high-temperature laminar jets. Zhurnal vychislitel'noy matematiki i matematicheskoy fiziki, v. 1, no. 5, 1961, 856-868.

Temperature profiles, velocity profiles, and the boundary of the mixing zone of a viscous compressible gas jet discharging into a surrounding medium (stagnant or moving) are given, and equations are

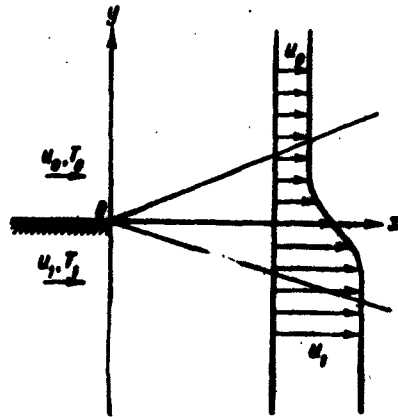


Fig. 9. Flow pattern of the mixing zone.

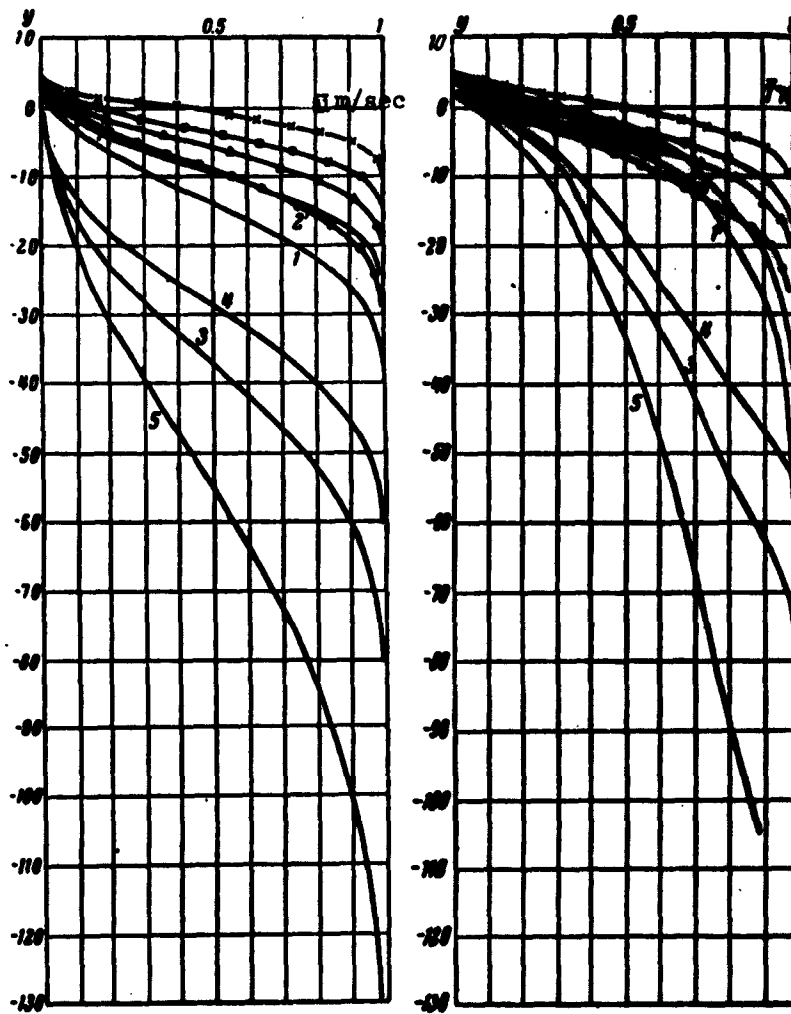


Fig. 10. Velocity \bar{u} and temperature \bar{T} profiles for the mixing of high-temperature and high-velocity gases with gases of low temperature and velocity

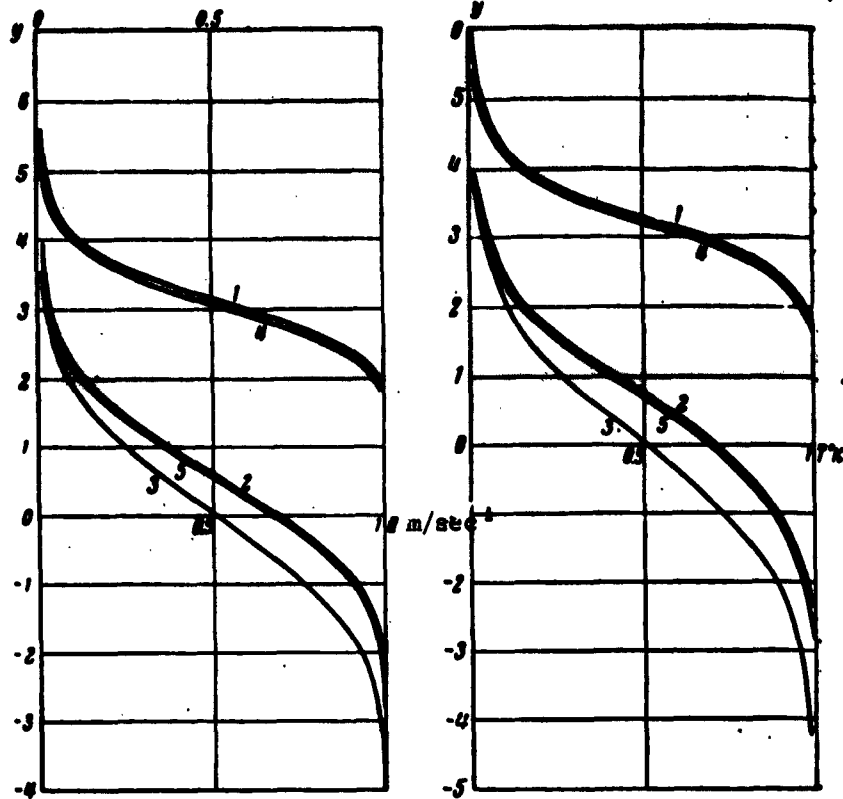


Fig. 11. Profiles \bar{u} and \bar{T} for the mixing of gases with small temperature differences ($T_0 = 273^\circ\text{K}$, $T_1 = 300^\circ\text{K}$) at $u_1 = 1000$ m/sec

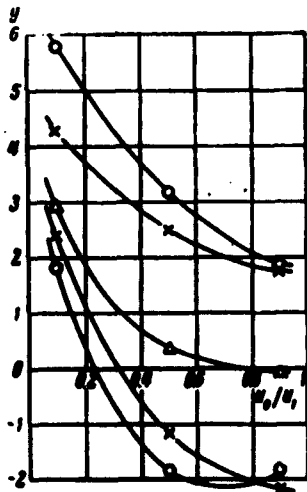


Fig. 12. Velocity and temperature profiles calculated for the mixing of cool high-velocity gases with a hot low-velocity gas

derived for determining the flow parameters. Because of high temperatures ($T > 2000^\circ\text{K}$), it is assumed that the Prandtl number

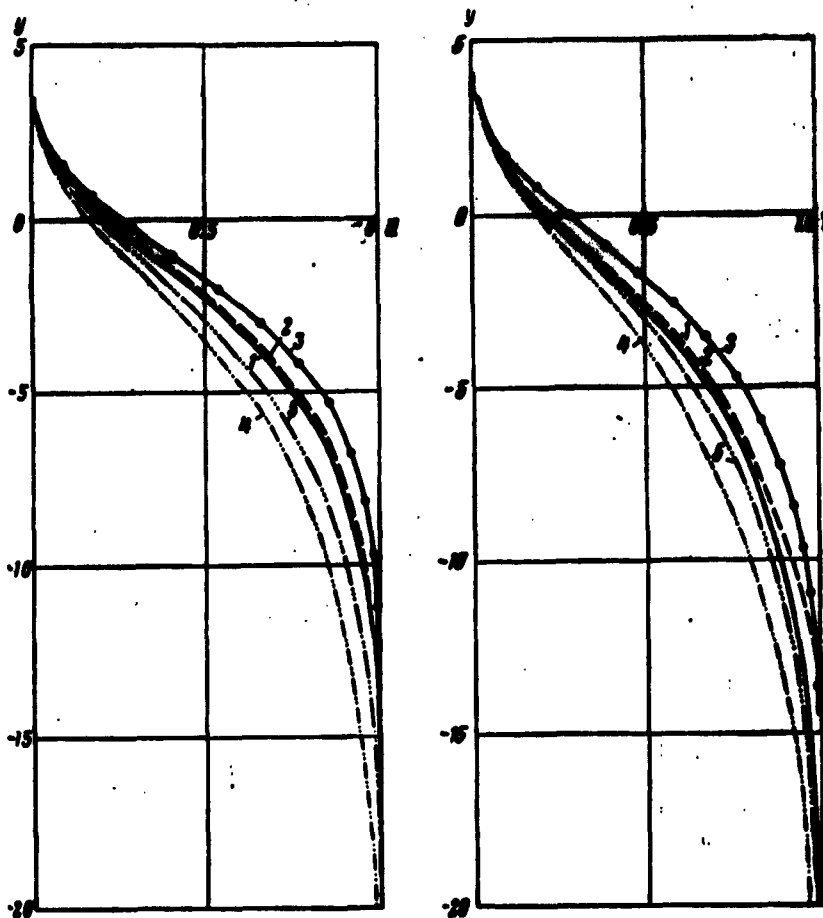


Fig. 13. Velocity and temperature profiles calculated for various cases of the mixing of cool high-velocity gases with hot low-velocity gases

changes with temperature and that the parameters (ρ - density, μ - viscosity, λ - heat transfer coefficient, C_p - specific heat capacity) are known functions of the temperature T . A numerical calculating method is given for the determination of temperature profiles and velocity profiles in the mixing zone of semi-infinite streams (see Fig. 9) at $U_0 = 100$ m/sec, $T_0 = 273^\circ\text{K}$, $u_1 = 1000$ m/sec, $T_1 = 10,000^\circ\text{K}$. The calculations were made with and without taking account of dissociation. The results obtained indicate the influence of dissociation on the width and position of the temperature- and velocity-mixing zones and also on the position of the zero line of the stream. Figs. 10-14 show the velocity \bar{u} and temperature T profiles for the mixing of high-temperature and high-velocity gases with

gases of low temperature and velocity; the dependence of these profiles on the ratio of the temperatures and velocities of the mixed gases is visible.

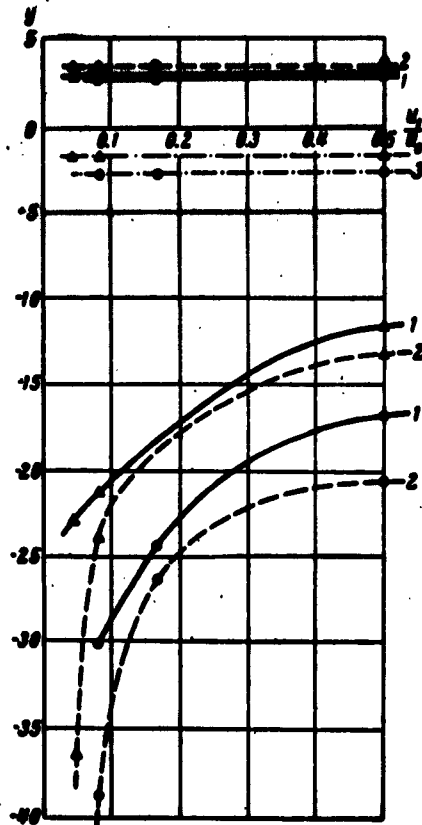


Fig. 14. Variation of the boundary of the mixing zone and of the neutral line of the stream described in Fig. 13 depending on the ratio of the velocities and temperatures of the mixed streams

5. Linkovskiy, G. B. Calculation of a noncylindrical ejector. *Inzhenerno-fizicheskiy zhurnal*, v. 2, no. 7, 1959, 87-91.

The principal difficulty in calculating an ejector with a noncylindrical mixing chamber (Fig. 15, a and b) is that in such a case the equation of momentum,

$$M_3 W - (m_{s1} W_1 + m_{s2} W_2) = \bar{p}(f_1 + f_2) - pF + \bar{R}$$

(where $M_3 = m_{s1} + m_{s2}$; m_{s1} is the mass flow rate of the ejecting and m_{s2} of the ejected liquid; W , w_1 , and w_2 refer to the flow velocities in the corresponding sections of the ejector; \bar{p} and p are the pressures in the corresponding sections of the ejector; f_1 , f_2 , and F refer to the areas of the cross sections 1-1, 2-2, and 3-3), incorporates an unknown term, \bar{R} , which refers to the force exerted on the flow by the wall of the ejector. To overcome this difficulty, an assumption was made that the pressure distribution along the ejector wall is linear. In this case the mean pressure (p_{av}) may be

determined as the arithmetic mean of the pressures at the inlet and exit of the mixing chamber,

$$p_{av} = \frac{\bar{p} + p}{2}, \text{ and } \bar{R} = p_{av} [F - (f_1 + f_2)].$$

A closed system of equations may thus be set up for the discharge from an ejector with a noncylindrical mixing chamber:

$$aW^3 + bW + c = 0.$$

where

$$a = (m_1 + m_2) \frac{f_1 + f_2 - 3F}{2(F + f_1 + f_2)},$$

$$b = \frac{2(m_1 W_1 + m_2 W_2)F}{F + f_1 + f_2} - \bar{p}F,$$

$$c = m_1 \left(\frac{p_1}{\rho_1} + \frac{W_1^2}{2} \right) + m_2 \left(\frac{p_2}{\rho_2} + \frac{W_2^2}{2} \right).$$

Using the expression $p_{av} = \frac{\bar{p} + p}{2}$ and disregarding the friction between the flow and the wall,² the following system of equations was set up for the pressure in a subsonic ejector:

$$ap^3 + bp + c = 0,$$

where

$$a = \frac{(F + f_1 + f_2)^3}{8M_1} - \frac{c_p F (F + f_1 + f_2)}{2gRM_1},$$

$$b = \frac{c_p F}{gRM_1} \left[\frac{(F + f_1 + f_2)\bar{p}}{2} + m_{21}W_1 + m_{22}W_2 \right] - \frac{(m_{21}W_1 + m_{22}W_2)(F + f_1 + f_2)}{2M_1} - \frac{(F + f_1 + f_2)^3 \bar{p}}{4M_1},$$

$$c = \frac{\left[\frac{(F + f_1 + f_2)\bar{p}}{2} + m_{21}W_1 + m_{22}W_2 \right]}{2M_1} - m_{21} \left(c_{p1}T_1 + \frac{W_1^2}{2g} \right) - m_{22} \left(c_{p2}T_2 + \frac{W_2^2}{2g} \right).$$

Both systems of equations have two roots; consequently, two values of p may be obtained, depending on the conditions at the exit of the ejectors.

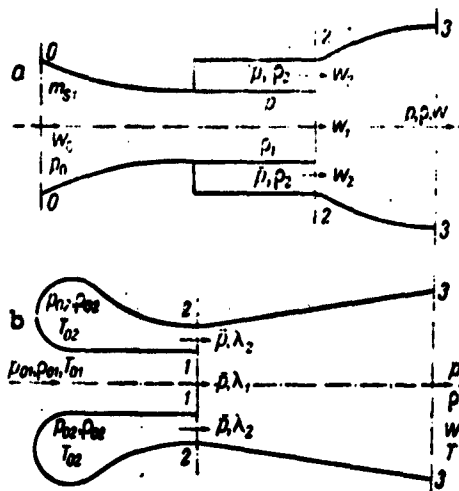


Fig. 15. a and b. Diagrams of noncylindrical ejectors

6. Popov, N. N. Mixing of gas streams. Izvestiya vysshikh uchebnykh zavedeniy. Aviatsionnaya tekhnika, no. 3, 1960, 80-86.

The interaction and mixing of two or more gas streams, e.g., in ejectors, combustion chambers, or afterburners, was studied using the multicomponent fluid model proposed by Kn. A. Rakhmatulli (Fig. 16). A general case of one-dimensional steady flow of a compressible gas is considered. The previously published system of equations obtained by Rakhmatulli for mixing of two incompressible gas streams,

$$\frac{\bar{p}_1}{p_1} + \frac{\bar{p}_2}{p_2} = 1,$$

$$f(x) u_{p_1} = C_1,$$

$$f(x) v_{p_2} = C_2,$$

$$u \frac{du}{dx} = -\frac{1}{\rho_1} \frac{d\rho}{dx} \frac{K}{\rho_1} (v - u),$$

$$v \frac{dv}{dx} = -\frac{1}{\rho_2} \frac{d\rho}{dx} \frac{K}{\rho_2} (u - v),$$

and the following four equations,

$$\rho_1 = \rho_1(x, y, z, t)$$

$$\rho_2 = \rho_2(x, y, z, t)$$

$$\frac{d}{dx} \left[C_1 \left(\frac{u^2}{2} + C_v T_1 \right) + f \cdot \rho u \right] = -f \cdot K \cdot (u - v)^2 + q - Q,$$

$$\frac{d}{dx} \left[C_2 \left(\frac{v^2}{2} + C_v T_2 \right) + f \cdot \rho v \right] = -f \cdot K \cdot (u - v)^2 + Q,$$

were used to obtain a closed system of equations for determining the following nine unknown functions; u , v , ρ_1 , ρ_2 , $\bar{\rho}_1$, $\bar{\rho}_2$, T_1 , T_2 , and p (where u and v are the velocities; ρ_1 and ρ_2 are densities; $\bar{\rho}_1$ and $\bar{\rho}_2$ are the corrected densities in the case of each gas occupying the entire volume; T_1 and T_2 are the temperatures of the two streams; and p is the total pressure). The other denotations in these equations are $f(x)$, the variable cross section of the channel; C_1 and C_2 , the flow rates of the gases per second; and K , the interaction function taking into account the effect of the gases on each other and must be determined experimentally. The system of equations, in some cases, may also be used for nonsteady flows giving a quasistationary approximation. The system of equations was solved approximately for the flow of a two-component gas stream obeying the equation of state of an ideal gas. The limiting velocity, which u and v approach at sufficiently high values of γx (where $\gamma = f(K_1/C_1 + K_2/C_2)$), is expressed by the equation:

$$V_{\infty} \cdot D_1 = \frac{\frac{K_2}{C_2} u_0 + \frac{K_1}{C_1} v_0}{\frac{K_1}{C_1} + \frac{K_2}{C_2}}.$$

In a particular case when the pressure change along the mixing zone is negligible, the latter equation assumes the following form:

$$V_{\infty} = \frac{C_2 u_0 + C_1 v_0}{C_1 + C_2}.$$

The solutions of the equations for the other unknown functions are also presented. It is shown that the theory describes correctly the mixing of two gas streams and may be generalized for the mixing of several streams.

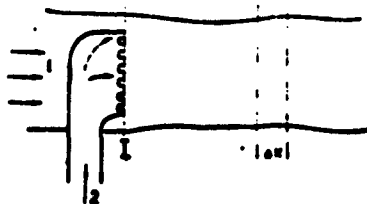


Fig. 16. Gas flow diagram

7. Shcherbina, Yu. A. The influence of initial turbulence on the boundaries and range of submerged jets. III: Moscow. Fiziko-tekhnicheskiy institut. Trudy, no. 7, 1961, 152-157.

A method is given for calculating the boundaries and range of submerged jets with an initial turbulence ranging from 6 to 30% by the semiempirical theory elaborated by V. Prandtl, V. Tolmin, and others and adapted by G. N. Abramovich for supersonic jets. Results of experimental investigation of plane submerged jets of various initial turbulences are also presented. The experimental unit (Fig. 17) consists of a pipe (length, 3000 mm; diameter, 200 mm) connected to a receiver with a plane nozzle (width, 250 mm; height, 24.6 mm). The turbulence of the jet was varied by the use of interchangeable grids in the nozzle. Air velocity was constant in all experiments, and a nearly rectangular velocity profile was maintained at the exit of the nozzle. Experimental results (Figs. 18--23) lead to the following conclusions: 1) The characteristics of highly turbulent jets (30% of turbulence) conform with the basic characteristics of jets with low turbulence. The velocity of jets remains self-similar (Fig. 18) along the length of the jet, and the lines of equal velocity (Fig. 19) remain rectilinear. 2) It is necessary to account for the increasing distance of the polar point of the jet from the nozzle exit. 3) In calculating the range of turbulent jets, it is necessary to account for the increasing coefficient of turbulence with the increasing initial turbulence.

The abstract employs the following conventional signs; a - empirical constant of turbulence; s - distance of the pole of the jet from the nozzle exit section; u - longitudinal velocity of the flow; u_0 - initial flow velocity; u_m - maximum flow velocity in a given section; $2b_0$ - height of the plane jet; y - coordinate of a point in which the velocity is equal to the half of the maximum velocity in a given section; x, y - rectangular coordinates; ϵ_0 - initial intensity of the jet.



Fig. 17. Diagram of the experimental device

1 - Pipe; 2 - receiver; 3 - nozzle.

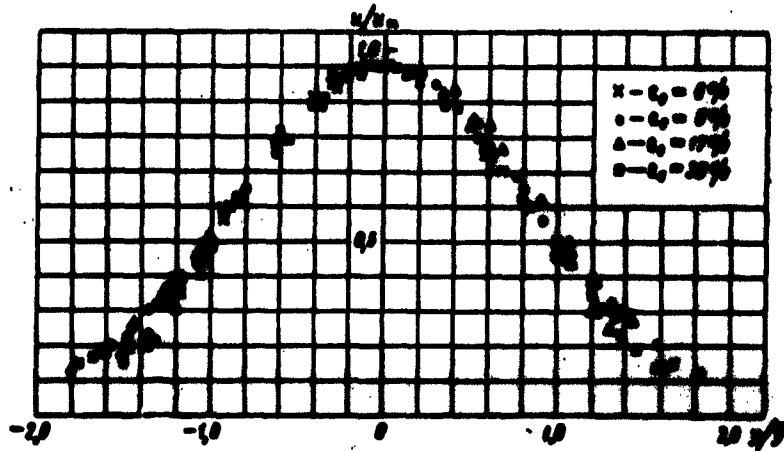


Fig. 18. Dependence of the dimensionless jet velocity on the dimensionless coordinate y at various distances from the nozzle ($x = 150, 400, 700$ mm)

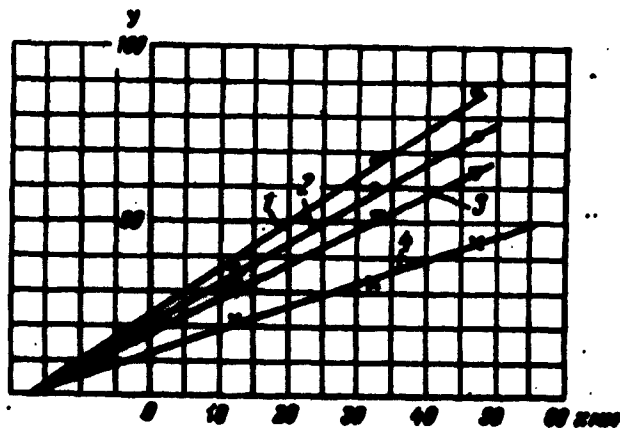


Fig. 19. Curves of equal dimensionless velocities in a jet with an initial turbulence $\epsilon_0 = 30\%$

1 - $u/u_m = 0.4$; 2 - $u/u_m = 0.5$;
 3 - $u/u_m = 0.6$; 4 - $u/u_m = 0.8$.

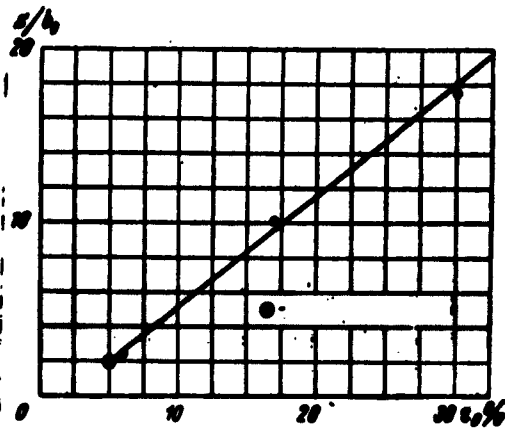


Fig. 20. Relative distance of the pole of the jet from the exit section of the nozzle, for jets with an increased initial turbulence

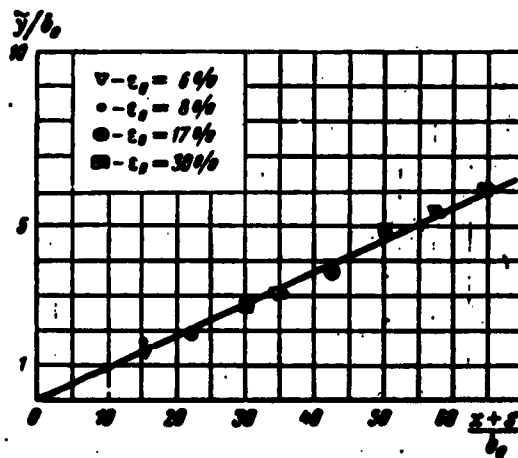


Fig. 21. Lines of dimensionless velocity; $u/u_m = 0.5$ for jets with various initial turbulences

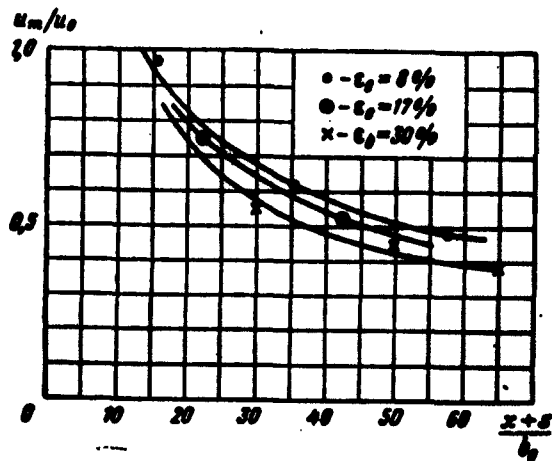


Fig. 22. Dimensionless axial velocity of jets with various initial turbulences

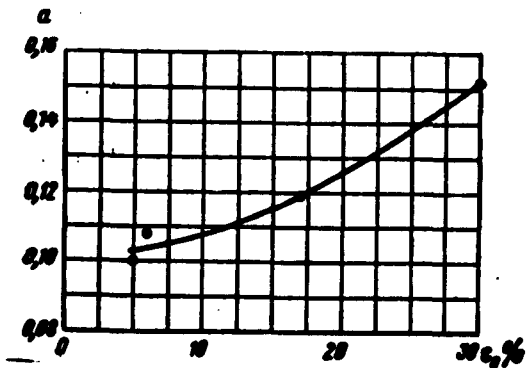


Fig. 23. Turbulence coefficient for jets with an increased initial turbulence

- d. Uryukov, B. A. The theory of a differential ejector. Zhurnal prikladnoy mekhaniki i tekhnicheskoy fiziki, no. 5, 1963, 41-47.

A differential ejector is analyzed and compared with single and multistage supersonic ejectors. The differential ejector (Fig. 24) may be considered as consisting of an infinite number of elementary ejectors. It is assumed in this analysis that 1) friction and heat transfer at the ejector walls are negligible; 2) the mixed gases are ideal and have the same chemical composition; and 3) velocity, temperature, and

pressure profiles are uniform in the initial section of each elementary ejector. The analysis is made in terms of dimensionless parameters

$$\lambda = \frac{w}{a_*}, \quad n = \frac{Q}{Q_*}, \quad \tau = \frac{T_0'}{T_0}, \quad \epsilon = \frac{P_0'}{P_0}, \quad \epsilon_* = \frac{P_0}{P_*}, \quad \varphi = \frac{r}{r_*}$$

where F is the surface; Q , the discharge rate; w , the velocity; T_0 , the stagnation temperature; P_0 , the pressure; λ , the reduced velocity; n , the injection coefficient; τ , the stagnation temperature drop; ϵ , the total pressure drop; ϵ_* , the pressure ratio; φ , the relative surface of the mixing chamber; and a_* , the critical sonic velocity. Subscripts 1 indicate conditions at the ejector exit and subscripts 0 indicate conditions at ejector inlet; dF' , dQ' , w' , T_0' , and P_0' denote the same parameters of the ejecting gas in the cross section of an elementary ejector; and df , the variation of the surface of an elementary ejector. If $\lambda < 1$ at the end of the mixing chamber, the losses in the diffuser are small. If $\lambda > 1$, various regimes are established in the diffuser. For larger values of λ , the losses are high. The determination of an optimum ejector is reduced to the determination of the distribution of velocities along the length of the ejector $\lambda = \lambda(n)$ and $\lambda' = \lambda'(n)$ at which ϵ_1 attains a maximum value. The optimum value of λ_1 , therefore, may be determined from the combined consideration of the ejector and diffuser. It may be demonstrated that λ_0 (at the inlet of the ejector) increases with increasing n . The optimum ejector corresponds to a constant $\lambda = \lambda_1$ along the lengths of the ejector. If $\lambda_{00} < \lambda_1$, the optimum ejector corresponds to $\lambda = \lambda_0$ at $\lambda_0 \leq \lambda_1$ and, therefore, $\lambda = \lambda_1$ to the end of the ejector.

The following cases are analyzed; a) $\lambda = \lambda_0$ and $\lambda' = \lambda_0'$ along the whole length of the ejector; b) $\lambda_1 < \lambda_{00}$ (the most interesting case for practical applications); and c) a differential ejector at $\tau = 1$, in which the surface of the mixing chamber does not change in each elementary ejector and λ' is constant. It is shown how the equations for an optimum ejector at $\lambda_1 > \lambda_0$ can be used for evaluating the influence of the gas temperature on the compression ratio of the ejector.

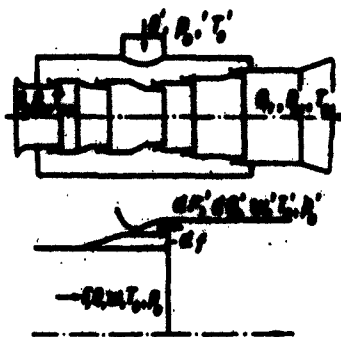


Fig. 24. Diagram of a differential ejector

9. Yakovlevskiy, O. V. Hypothesis on the generalization of ejection characteristics of turbulent gas jets and its application. IN: Akademiya nauk SSSR. Izvestiya. Otdeleniye tekhnicheskikh nauk. Mekhanika i mashinostroyeniye, no. 3, 1961, 40-54.

Starting from the assumption that the impulse in the initial section of a nozzle is the basic characteristic of a turbulent jet, the following hypothesis has been postulated: If two turbulent jets discharging from identical nozzles have equal impulses in their initial cross sections, then both jets have the same ejection properties (i.e., drawing of the neighboring fluid by the jets is governed by the same law), expressed by the following dimensionless equation:

$$\frac{dG_1}{dx} = \sqrt{\rho} \frac{dG_0}{dx} \quad (G = \frac{G}{G_0}, x = \frac{x}{r_0})$$

where G is the mass flow rate of a gas in an arbitrary cross section; a and i refer to the arbitrary submerged isothermal jets and to a standard one, respectively; ρ is the density; x is the longitudinal coordinate; and r_0 is the initial radius of an axisymmetrical jet. On the basis of this hypothesis, ejection properties of any arbitrary jet may be determined by determining the ejection properties of a corresponding turbulent jet of an incompressible fluid, using the equations derived for the initial section of an arbitrary jet.

$$G = \sqrt{\rho} r_0^2 + 1$$

and for the main section of an axisymmetrical jet:

$$G^0 = \sqrt{\rho^0} \alpha_1 (x^0 + \beta_1)$$

The flow diagrams in the initial section of a jet mixing zone and in the main section of a jet discharging into a coaxial flow are given in Figs. 25 and 26. Together with the previously derived equations for the conservation of momentum and for enthalpy, the new equation forms a closed system of equations for calculating gas jets discharging into a moving medium. The application of the proposed hypothesis is illustrated by calculating various parameters for the initial section of a jet in a coaxial flow, for a turbulent heated gas jet (with varying thermodynamic parameters) in a coaxial flow, for a jet of an incompressible fluid, for a supersonic jet under design and off-design flow regimes, and for a gas liquid jet. Comparison of the calculated data with published experimental data shows good agreement.

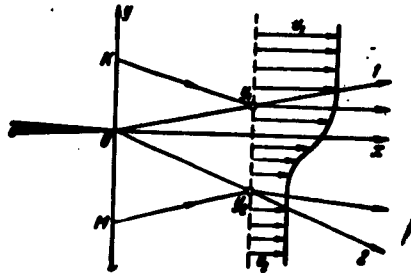


Fig. 25. Flow diagram of the initial section of a jet mixing zone

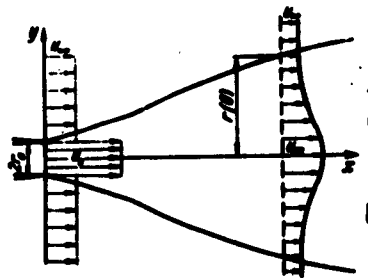


Fig. 26. Flow diagram of the main section of a jet discharging into a concurrent flow

10. Yakovlevskiy, O. V. Thickness of the turbulent mixing zone on the boundary of two streams of gases of different velocities and densities. IN: Akademiya nauk SSSR. Izvestiya. Otdeleniye tekhnicheskikh nauk, no. 10, 1958, 153-155.

The effect of temperature and velocity on the angular coefficient (b^*) of the widening of the turbulent mixing zone of two nonisothermal gas streams was studied experimentally and theoretically. The experimental data obtained (Fig. 27) show that at $m = 0$ ($m = u_2/u_1$, where u_2 and u_1 refer to the velocities of the two streams), b^* depends markedly on the ratio of the densities of the two streams r ($r = \rho_2/\rho_1$), and, therefore, the published equation for calculating b^* is not applicable to nonisothermal streams. The following semiempirical equation for determining b^* has been derived:

$$b^* = c \frac{1+r}{2} \cdot \frac{1-m}{1+rm}$$

where the constant c is determined experimentally. Reduction of the experimental data in b^* , r coordinates showed that for submerged ($m = 0$) jets of a compressible gas, b^* may be calculated using the following equation: $b^*_{m=0} = 0.27(1 + r/2)$, where r (at $m = 0$) is determined from the known equation:

$$r = 0^{\circ} \frac{1 - a\lambda_1^2}{1 - a\lambda_1^2 m^2} \quad \left(0^{\circ} = \frac{T_1^{\circ}}{T_2^{\circ}}, \quad a = \frac{k-1}{k+1}, \quad k = \frac{c_p}{c_v} \right)$$

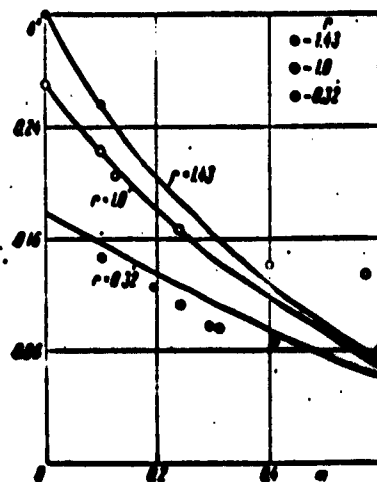


Fig. 27. The dependence of the angular coefficient of the widening of the mixing zone of two nonisothermal gas streams on the ratios of the velocities (m) and densities (r) of the two streams

INQUIRY ON AVAILABILITY OF TRANSLATIONS

I am interested in availability of translations of the sources indicated below (please enter reference numbers given in the Table of Contents).

Return this form to the local monitor of the ARPA-ATD project or mail it directly to:

Head, Science and Technology Section
Aerospace Technology Division
Library of Congress
Washington, D. C. 20540

ATD DISTRIBUTION LIST
FOR 1961-1962

<u>ORGANIZATION</u>	<u>No. of Copies</u>
NASA(AFSS-1)	1
NASA(Tech. Lib.)	1
DDC	20
DIA(DD/DIA/SA/GI)	4
CIA(SD)	3
Gen. Ast. Res. Corp.	1
Nat. Sci. Found.	1
DIA	1
RAND	1
SAK/DL-510	2
AMXST-SD-TD	5
CIA(OCR-STAN. DIST)	6
AFTAC/IG-I)	1
Env. Res. Asc.	1
Tech. Doc.	1
AEDC(AEY)	1
Nat. Bur. Stand.	1
ESD(ESY)	2
ESD(ESTI)	1
ASD(ASF)	1
McGraw-Hill	10
TDBTL (Tech. Lib.)	5
TDBXP	3
AIR UNIVERSITY	1
U.S. Naval S & T Intell. Center	3
AFCRL (CRTEF)	3
ARL (ARI)	1
OAR (RRY)	3
FTD (TDEP)	1
Office of Research Analyses	1